Evaporation from a Two-Dimensional Meniscus

V. A. Wehrle* and G. Voulelikas†
Communications Research Centre, Ottawa, Canada

Evaporation from a two-dimensional meniscus, caused by the heating of a flat platinum plate immersed vertically in a pool of water, is modeled and analyzed. Bernoulli's equation for incompressible inviscid fluid flow is applied to the meniscus line, which is approximated to be a streamline of the liquid flow. The effects on evaporation heat transfer of two types of resistance are examined parametrically: 1) that due to the evaporation coefficient at the liquid-vapor interface, and 2) that due to the presence of a nonevaporating thin film at the wall. A logarithmic coordinate transformation is used to stretch the region in the neighborhood of the wall, and the numerical results show that in this region the velocity at, and heat flux through, the meniscus line have maximum magnitudes. Using physically plausible values for resistance of the first type, the numerical results show that both the local and the total Nusselt numbers are insensitive to all physically plausible values for resistance of the second type. If, on the other hand, resistance of the first type is ignored altogether, serious errors can arise in the computed values for the total Nusselt number.

Nomenclature

a = arc length, cm
g = gravitational acceleration, cm/s^2
k = thermal conductivity, W/cmK
M = molecular weight, g/gmole
$\dot{m}$ = liquid mass flow rate per unit depth of meniscus, g/cm s
Nu_ℓ = local Nusselt number
p = pressure, N/cm^2
q = local heat flux, W/cm^2
$\bar{R}$ = universal gas constant, J/gmoleK
R_m = interface evaporation resistance, cm^{2}K/W
T = temperature, K
u = dimensionless velocity at the meniscus line
V = velocity at the meniscus line, cm/s
$\bar{V}$ = average radial velocity, cm/s
x,y = Cartesian coordinates
α,β,γ = constants defined by Eq. (8)
Γ = dimensionless mass flow rate through the arc, subtended by the wedge angle, under the meniscus line
ΔT = temperature difference between wall and vapor, K
ϵ = thickness of nonevaporating thin film at the wall, cm
ζ = height of meniscus line at any point x, cm
η = dimensionless coordinate defined by Eq. (5)
θ = wedge angle between the wall and the tangent to the meniscus line, rad
κ = curvature of meniscus line, cm^{-1}
λ = latent heat of evaporation, J/g
μ = viscosity, g/cm s
ρ = density, g/cm^3
σ = surface tension, dyne/cm
$\bar{\sigma}$ = evaporation coefficient
ϕ = dimensionless height of the meniscus line
χ = variable defined in Eq. (5)

Subscripts

m = meniscus
v = vapor
w = plate wall

Introduction

IN many heat-transfer problems involving liquid-vapor phase change processes, the phenomena associated with evaporation from a curved meniscus are important. For example, and the prime motivation for this investigation, the evaporating meniscus is a limiting factor in the overall performance of heatpipes.

Several models have been presented and analyzed on the heat transfer which occurs in a curved meniscus. Some models ignore all resistances to heat flow in the meniscus other than that due to the thickness of the liquid. Not surprisingly, these tend to yield very high, if not singular, values of heat transfer in the immediate neighborhood of the meniscus cusp where the thickness of the liquid approaches zero. For example, Berger and Feldman[1] performed a finite difference analysis of the heat transfer characteristics of V-groove and rectangular-groove heatpipes, and from their numerical results observed that the majority of the heat transfer does indeed occur at and near the meniscus cusp. While their predictions for the overall heat-transfer coefficient yielded reasonably good agreement with experiments, their calculations were criticized by Schneider et al.[2] because, in the dominating region of the cusp, their numerical grid was very coarse. In the Schneider et al. paper, a similar physical model was analyzed using the finite element method. The authors gave careful attention to mesh-generation schemes which facilitated convergence of the calculations, and predicted values for the overall heat transfer coefficient which were substantially higher than those of Berger and Feldman. An analytical approach to the same problem was taken by Edwards et al.,[3] who attempted to account also for variations in the radius of curvature of the meniscus due to variations in the local liquid pressure distribution. The power-law form of their analytical solution yields singular behavior of the liquid-vapor pressure difference at the cusp of the meniscus, which implies negative absolute liquid pressures at and near the cusp, a physical impossibility. In order to facilitate their analytical solution, the authors linearized the differential equation for the radius of curvature by ignoring a term in the slope of the meniscus profile. However this approximation must be considered poor, because singular behavior of the liquid-vapor pressure

Presented as Paper 83-1526 at the AIAA 18th Thermophysics Conference, Montreal, Canada, June 1-3, 1983; received June 24, 1983; revision received May 10, 1984. This paper is declared a work of the Canadian Government and therefore is in the public domain.

*Thermal Engineer, Space Mechanics Directorate, Department of Communications.

†Junior Thermal Engineer, Space Mechanics Directorate, Department of Communications.

difference also implies rapid change in the slope of the meniscus profile.

An additional resistance to the flow of heat in a meniscus exists at the liquid-vapor interface, and its presence was discovered by experiments in the early 1900's (a review of this work is given in Jakob[4]). This resistance can be expressed in terms of an "evaporation coefficient," and causes a temperature difference to exist between a liquid and its saturated vapor at any pressure below the critical point. A summary of the associated theory is given by Sukhatme and Rohsenow,[5] and a compilation of evaporation coefficients for several materials is given by Paul.[6]

Another resistance to the flow of heat in a meniscus can arise due to the presence of a nonevaporating thin film at the wall. As discussed by Read and Kitchener,[7] the existence and thinness of such a film has less to do with simple capillary theory than with a complex theory involving several types of intermolecular forces. A theoretical treatment of the subject of thin films is given by Sheludko.[8] The impact of a nonevaporating thin film, if it exists for a particular wall/liquid combination, is that it precludes singular behavior of the local heat transfer at the cusp of the meniscus.

Potash and Wayner[9] evolved a model of heat transfer in a curved meniscus which included, in addition to the usual liquid thickness resistance, the effects of both the interface evaporation resistance and the nonevaporating thin-film resistance. Applying their model to the case of a flat glass plate immersed in a pool of saturated carbon tetrachloride, they obtained numerical results for the variation of the local heat transfer, amongst other parameters, with respect to distance from the wall. However, their model yielded negative absolute pressure in the liquid at the cusp of the evaporating portion of the meniscus; a physical impossibility. Also, because they did not study the effects of interface evaporation resistance and nonevaporating thin-film resistance parametrically, it is not yet clear what relative importance is to be attached to each resistance component.

In the following sections, a new model for evaporation from a curved meniscus is developed, and is employed to examine parametrically the relative influence of interface evaporation resistance and nonevaporating thin-film resistance.

Mathematical Model

Bernoulli's equation for steady incompressible fluid flow can be applied to the meniscus line, just on the liquid side of the liquid-vapor interface, if it can be assumed that 1) the meniscus line is a streamline of the liquid flow, and 2) viscous dissipation at this streamline is negligible. Evaporation from the meniscus line entails mass transfer across it, which implies that this line cannot be a true streamline of the liquid flow. Hence, the first assumption implies an approximation of the true physical situation. As is discussed in the next section on the velocity model, the second assumption is valid. Applying Bernoulli's equation to the meniscus line,

$$\frac{p}{\rho g}+\zeta+\frac{V^2}{2g}=H_0$$

where H_0 is a constant, and $y=\zeta(x)$ is the equation of the meniscus line (see Fig. 1). Because the meniscus line is defined to be just on the liquid side of the liquid-vapor interface, it is understood that all fluid properties and parameters apply to the liquid phase unless otherwise subscripted. The pressure drop across a two-dimensionally curved meniscus is given in terms of the surface tension and local curvature as $(p_v-p)=\sigma\kappa$, so that

$$\frac{1}{\rho g}(p_v-\sigma\kappa)+\zeta+\frac{V^2}{2g}=H_0$$

Now as $x\to\infty$, $\kappa\to 0$, $\zeta\to 0$, and $V\to 0$. If we make the usual assumption that the vapor pressure above the meniscus line is constant, it follows that $H_0=p_V/\rho g$. Noting that the local curvature κ is related to the local geometry of the meniscus line through the differential equation

$$\kappa=\zeta''/(1+\zeta'^2)^{3/2}$$

where the prime denotes differentiation with respect to x, we obtain

$$\frac{\zeta''}{(1+\zeta'^2)^{3/2}}-\frac{\rho g}{\sigma}\left(\zeta+\frac{V^2}{2g}\right)=0$$

If there does exist a nonevaporating thin film of thickness ϵ at the wall (see Fig. 1), then the appropriate boundary conditions are

$$\zeta'(\epsilon)=-\cot\theta_\epsilon, \qquad \zeta(\infty)=0$$

where θ_ϵ is the contact angle for the given wall/liquid material combination. The second-order differential equation in ζ can be rendered somewhat cleaner as two first-order differential equations by substitution of the geometrical relationship $\zeta'=-\cot\theta$. The equivalent two first-order equations are

$$\theta'-\frac{\rho g}{\sigma\sin\theta}\left(\zeta+\frac{V^2}{2g}\right)=0, \qquad \zeta'+\cot\theta=0 \tag{1}$$

with boundary conditions $\theta(\epsilon)=\theta_\epsilon$, $\zeta(\infty)=0$.

Velocity Model

Equations (1) are not yet integrable because the dependency of V on x is not yet defined. Sparrow and Starr[10] obtained an analytical solution for the velocity distribution in a wedge channel, assuming the flow to be radial, fully developed, and laminar. We shall assume that their solution can be applied for each "local wedge" of half-taper angle θ_i defined by the intersection of the vertical wall and the tangent to the meniscus line at the local point i of interest (see blowup in Fig. 1). Thus, the velocity at the meniscus line V, normalized with respect to the average radial velocity $\bar{V}$ through the arc under the meniscus line, is

$$\frac{V}{\bar{V}}=\frac{1-\cos\psi}{(\sin\psi/\psi)-\cos\Psi}$$

where $\psi=2\theta\{1-\delta\Gamma/4\theta\}^{1/2}$ and $\delta=\bar{\epsilon}k\Delta T/\mu\lambda$. This formulation is valid for $\delta\Gamma/4\theta<1$, which is the case for all results presented in this paper. Here Γ is a nondimensionalized mass flow rate [defined in Eq. (5)], and the parameter $\bar{\epsilon}$ in the definition of δ is a linearization weighting factor as described by Sparrow and Starr and is a rather complicated function of

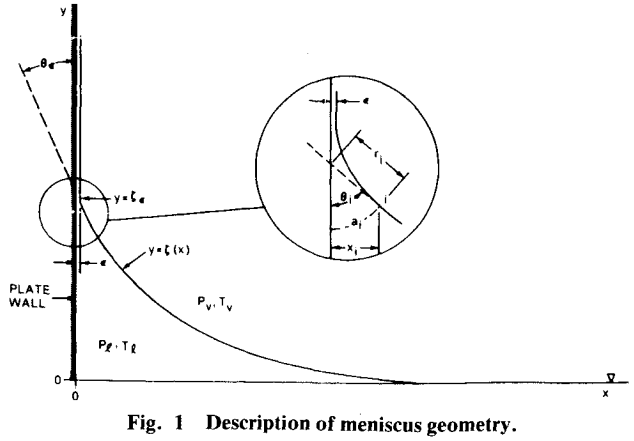

Fig. 1 Description of meniscus geometry.

ψ. Its value varies between 1.714 and 2.0 over the full possible range of ψ. Over our entire integration domain, the extent of which is chosen sufficiently large to satisfy adequately the outer boundary condition $\zeta(\infty)=0$, all our results show that $\delta\Gamma/4\theta$ is, in fact, much smaller than unity (always less than 0.0022). Hence, we may approximate $\psi=2\theta$ and, after some trigonometric manipulation, we obtain

$$\frac{V}{\bar{V}}=2\Big/1+\frac{\cot\theta}{\theta}\,(1-\theta\cot\theta)$$

In the local wedge model the flow is assumed to be radial, so that $\bar{V}=\dot{m}/\rho a$ where $\dot{m}$ is the mass flow rate, per unit depth of meniscus, through the circular arc under the meniscus line. The arc length through the wedge angle θ is given by simple geometry considerations as $a=x\theta/\sin\theta$, so that

$$V=\frac{2\dot{m}\sin\theta}{\rho x[\theta+\cot\theta(1-\theta\cot\theta)]} \tag{2}$$

It can be shown that the velocity V is related to the liquid pressure p at the meniscus line by

$$V=\{2[(p_v-p)/\rho-g\zeta]\}^{1/2}$$

Since p cannot be less than zero, it follows that a constraint on the magnitude of the meniscus line velocity is

$$V\le\{2(p_v/\rho-g\zeta)\}^{1/2}$$

For all our results, the constraint is not violated.

It can be demonstrated easily from the Sparrow and Starr full solution that the gradient of velocity with respect to arc length is exactly zero at the meniscus line. Hence, the second assumption, in the previous section on mathematical model, is entirely valid within the context of the local wedge velocity model.

Mass Model

Equation (2) requires an expression for $\dot{m}$, which is simply equal to the rate at which mass is evaporated at the meniscus line from all points between the nonevaporating thin film and the local point of interest. That is,

$$\dot{m}=\frac{1}{\lambda}\int_{S(\epsilon)}^{S(x)} q\,dS$$

where q is the local heat flux at the meniscus line and dS is an element of length along the meniscus line. We may write $q=\Delta T/R$, where $\Delta T=(T_w-T_v)$ is the temperature difference between the wall and the vapor, and R is the local resistance to heat flow. Now we shall attribute to R a "liquid path" component $(=a/k)$ and a "meniscus" component $(=R_m)$, these being in series. Noting that $dS=dx/\sin\theta$, we obtain

$$\dot{m}=\frac{1}{\lambda}\int_{\epsilon}^{x}\frac{k\Delta T}{x\theta+kR_m\sin\theta}\,dx$$

Table 1 Parametric values used in numerical analysis

$\bar{\sigma}$	Comment	ϵ, cm	Comment
0.04	Most probable value	10^{-5}	Thick film
		10^{-7}	Thin film
1.0	Maximum possible value	10^{-9}	No film[a]

[a] This dimension is less than the diameter of a water molecule.

It is more convenient, in terms of a numerical solution to the problem, to recast the $\dot{m}$ equation in differential form. Hence,

$$\dot{m}'=\frac{k\Delta T}{\lambda[x\theta+kR_m\sin\theta]} \tag{3}$$

with the boundary condition $\dot{m}(\epsilon)=0$. In this equation, the resistance R_m can be obtained from Sukhatme and Rohsenow[5] as

$$R_m=\frac{2-\bar{\sigma}}{\bar{\sigma}\lambda^2}\left(\frac{\pi}{2}\right)^{1/2}\left(\frac{\bar{R}}{M}\right)^{3/2}\frac{T_v^{5/2}}{p_v} \tag{4}$$

where $\bar{\sigma}$ is the evaporation coefficient for the given liquid. A compilation of values of $\bar{\sigma}$ for several materials is given by Paul.[6] Equation (4) is valid providing that the temperature difference (T_m-T_v) between the meniscus line and the vapor is small, and that the following condition is satisfied:

$$\frac{q}{\rho\lambda(2\bar{R}T_v/M)^{1/2}}<0.1$$

For all results presented in this paper we have set $(T_w-T_v)=1\,^\circ\mathrm{C}$, so that $(T_m-T_v)\le 1\,^\circ\mathrm{C}$. Also, the inequality condition is always satisfied.

Nondimensionalization

Equations (1-4) constitute a closed model of the evaporation heat transfer from a two-dimensional meniscus. As discussed in the introduction section, it is known that the local heat flux q has maximum magnitudes in the immediate vicinity of the cusp of the meniscus, and one suspects that the velocity along the meniscus line V will have similar characteristics. We are moved, therefore, to introduce a logarithmic coordinate transformation to stretch the region near the wall, and thereby to facilitate the numerical integration of the system of equations. We introduce, also, nondimensionalizations of the dependent variables. Let

$$\eta=\ell n\frac{x}{\epsilon},\quad \phi=\frac{\zeta}{\zeta_0},\quad \Gamma=\frac{\lambda\dot{m}}{k\Delta T},\quad u=\frac{V}{(2g\zeta_0)^{1/2}},$$
$$Nu_{,\ell}=\frac{\zeta_0 q}{k\Delta T},\quad \chi=\frac{\epsilon e^{\eta}}{\zeta_0\sin\theta} \tag{5}$$

By substitution into Eqs. (1-3) the differential equations and associated boundary conditions become

$$\dot{\theta}-\alpha\chi(\phi+u^2)=0,\quad \dot{\phi}+\chi\cos\theta=0$$
$$\dot{\Gamma}-\chi Nu_{,\ell}=0,\quad \theta(0)=\theta_\epsilon,\quad \phi(\infty)=0,\quad \Gamma(0)=0 \tag{6}$$

The dot denotes differentiation with respect to η, and the functional parameters u and $Nu_{,\ell}$ are

$$u=\frac{\beta\Gamma}{\chi[\theta+\cot\theta(1-\theta\cot\theta)]},\quad Nu_{,\ell}=\frac{1}{\chi\theta+\gamma} \tag{7}$$

The constants in this system of equations are given by

$$\alpha=\frac{\rho g\zeta_0^2}{\sigma},\quad \beta=\frac{2k\Delta T}{\rho\lambda\zeta_0(2g\zeta_0)^{1/2}},\quad \gamma=\frac{kR_m}{\zeta_0} \tag{8}$$

It is pointed out that the normalization constant ζ_0 in Eqs. (5) and (8) is the maximum height of the meniscus for the static case when $\Delta T=0$, and is given (see Batchelor,[11] for example)

by

$$\zeta_0 = \{2\sigma(1-\sin\theta_\epsilon)/\rho g\}^{1/2}$$

As well as the local meniscus Nusselt number $Nu,_\ell$ we find it informative to show results for the total meniscus Nusselt number $Nu,_{\text{tot}}$ defined by

$$Nu,_{\text{tot}} = \frac{Q_{\text{tot}}}{k\Delta T} = \frac{\lambda \dot{m}_{\text{tot}}}{k\Delta T} = \Gamma_{\text{tot}}$$

where Q_{tot} is the total heat flow, per unit depth of meniscus, through the meniscus line. Now Γ increases indefinitely with integration on x, and is proportional to $\ell n(x)$ for large x. Hence, if we wish to talk about a finite total meniscus Nusselt number, it is necessary to specify a criterion regarding the finite portion of the meniscus over which $Nu,_{\text{tot}}$ is defined. We have arbitrarily defined $Nu,_{\text{tot}}$ in terms of that portion of the meniscus for which the height of the meniscus line is greater than or equal to 1% of the maximum height of the meniscus line. Hence $Nu,_{\text{tot}} = \Gamma(\phi = 0.01)$.

Numerical Results and Discussion

The system of differential equations and associated definitions, Eqs. (4-8), was solved numerically using Gear's method (a variable order Adams predictor-corrector method of the implicit linear multistep type). Our computations were performed using the physical properties of water at 20°C; the significance of the plate material is manifested only through the value of the contact angle, which for water on platinum is 40 deg. The values of $\bar{\sigma}$ and ϵ, which are measures of the interface evaporation resistance and nonevaporating thin-film resistance, respectively, were varied parametrically as per Table 1. We do not know, nor are we concerned, whether or not there actually exists a nonevaporating thin film for water on platinum. The range of ϵ in Table 1 is intended merely to encompass values of ϵ typically observed for other material combinations (see Read and Kitchener[7] and Sheludko[8]). We also computed a complete set of solutions for $\Delta T = (T_w - T_v)$ equal to 1, 2, and 3°C. However, except for a simple multiplicative effect on u, this parameter did not change noticeably any of the curves presented in this paper; therefore, all our plots are for $\Delta T = 1$°C.

Figure 2 shows the dimensionless meniscus height ϕ, whose profile is found to be insensitive to any combination of the parameters in Table 1. This is not surprising, because in all of our results $u^2 \ll \phi$ so that the meniscus profile is essentially determined by only the first two equations in Eqs. (6), and is practically insensitive to the mass and heat transfer phenomena embodied in the third equation of Eqs. (6). Figure 2 also shows the local Nusselt number profiles, and these are found to depend strongly on the value of $\bar{\sigma}$ while being insensitive to the value of ϵ. In particular, the maximum value of $Nu,_\ell$ corresponding to the most probable value of $\bar{\sigma}$ is nearly two orders of magnitude less than the value corresponding to the maximum possible value of $\bar{\sigma}$. The results show that $Nu,_\ell$ asymptotes to a maximum value at the tip of the meniscus cusp, unlike the results of Potash and Wayner[9] who show, in their Fig. 3, that the local heat flux goes to zero there. The commencement of the descending portion of the $Nu,_\ell$ profile is an indication of the growing domination of liquid-thickness resistance over interface evaporation resistance. It follows, as is shown in Fig. 2, that the commencement point begins at smaller values of x for the lower resistance case of $\bar{\sigma} = 1.0$.

The dimensionless meniscus line velocity profiles for $\bar{\sigma} = 0.04$ and 1.0 are shown in Figs. 3 and 4, respectively. The bumps in the profiles are attributed to the lack of a sufficient number of significant digits, when x is very small, in the terms which make up the algebraic equation for u. Integration of the system of equations begins at $x = \epsilon$ (i.e., $\eta = 0$), and, hence, the phenomenon is more pronounced in the solutions for smaller values of ϵ. It is interesting to observe that while u is zero at the very tip of the meniscus cusp, it grows rapidly to a maximum value that is dependent on the value of ϵ, and then subsides along a profile path that is common for all values of ϵ. As is expected, Figs. 3 and 4 show that a larger $\bar{\sigma}$ (i.e.,

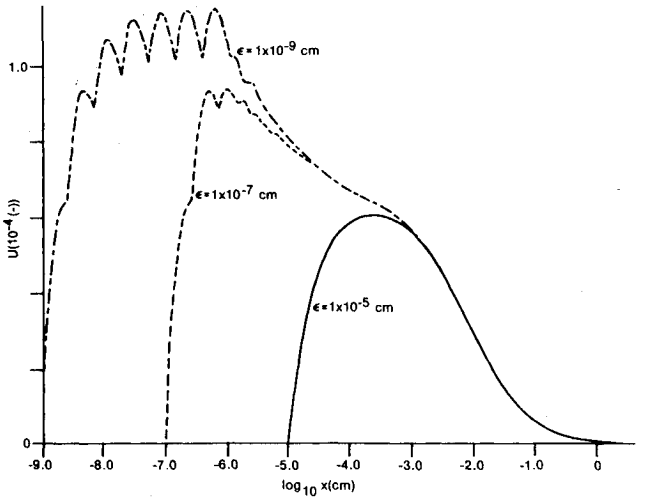

Fig. 3 Meniscus line velocity profiles for $\bar{\sigma} = 0.04$.

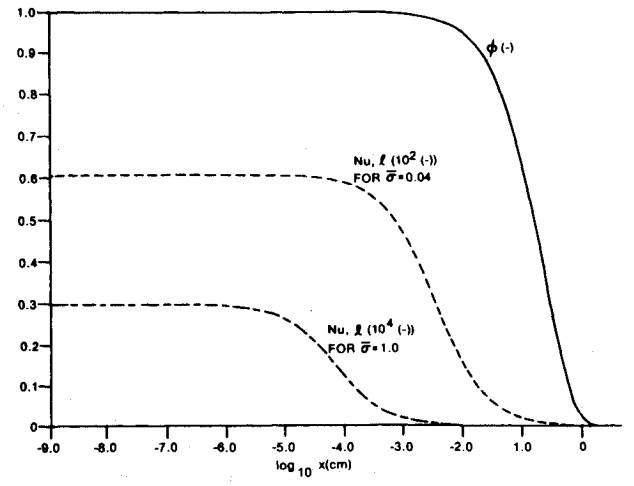

Fig. 2 Meniscus line height and local Nusselt number profiles. These curves do not noticeably change for 10^{-9} cm $\leq \epsilon \leq 10^{-5}$ cm.

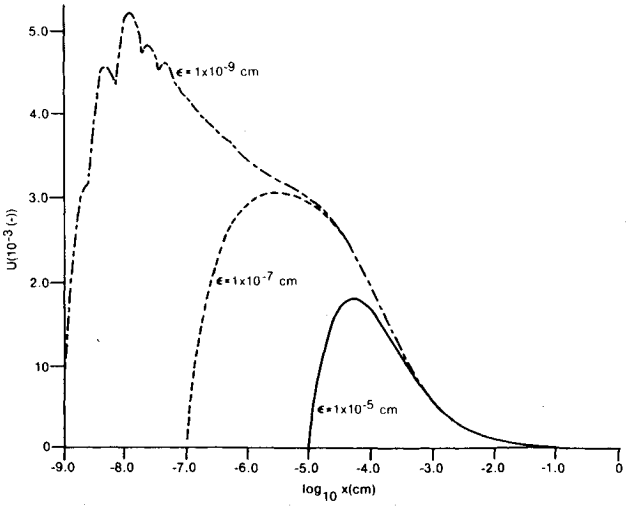

Fig. 4 Meniscus line velocity profiles for $\bar{\sigma} = 1.0$.

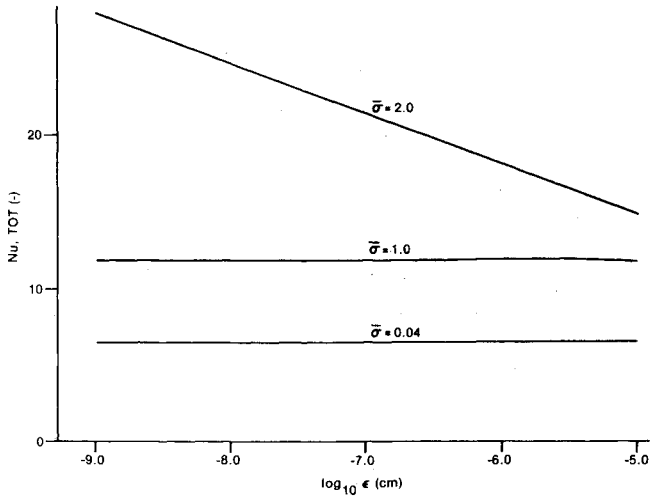

Fig. 5 Variation of total meniscus Nusselt number with $\bar{\sigma}$ and ϵ.

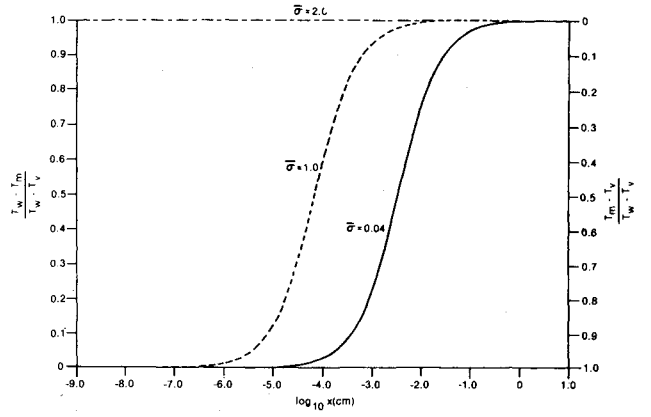

Fig. 6 Meniscus line temperature profiles. These curves do not noticeably change for 10^{-9} cm $\leq \epsilon \leq 10^{-5}$ cm.

smaller R_m) yields a larger maximum magnitude of u for any particular ϵ. In fact, we ran a case with $\bar{\sigma}=2.0$ (which is theoretically impossible, but renders $R_m=0$), and found that the velocity u grew very large with decreasing ϵ. In particular, for $\epsilon<10^{-8}$ cm, the velocity constraint following Eq. (2) is violated, a violation which was observed to occur in the numerical results given by Potash and Wayner.[9]

The effects of $\bar{\sigma}$ and ϵ on the integrated heat transfer parameter $Nu_{,\text{tot}}$ are shown in Fig. 5. It is clear that ϵ plays practically no role in the value of $Nu_{,\text{tot}}$ for all physically possible values of $\bar{\sigma}\leq 1$. However, if R_m is ignored altogether (i.e., $\bar{\sigma}=2.0$), then $Nu_{,\text{tot}}$ increases indefinitely with decreasing ϵ, although the interpretation of the results for $\epsilon<10^{-8}$ cm becomes difficult because, as mentioned previously, the velocity constraint following Eq. (2) is then violated.

In Fig. 6 we show a breakdown of $(T_w - T_v)$, a fraction of the drop occurring between the wall and the meniscus line and the remainder between the meniscus line and the vapor. One observes that interface evaporation resistance dominates near the wall, resulting in a meniscus line temperature practically equal to the wall temperature. However, the meniscus liquid thickness increases with increasing x, and the associated increasing resistance results in a meniscus line temperature which increasingly approaches that of the vapor.

We note, finally, that although this paper presents numerical results for the particular case of a platinum plate immersed in water, the model itself is equally applicable to other plate/liquid combinations. It was our experience, however, that property data (especially contact angle θ_ϵ and/or evaporation coefficient $\bar{\sigma}$) was not readily available for the more common plate/liquid combinations such as, for example, are typically employed in heatpipes.

Conclusions

In this paper we developed a new model, based on Bernoulli's equation applied to the meniscus line, for evaporation heat transfer from a two-dimensionally curved meniscus. We examined parametrically the relative influence of interface evaporation resistance and nonevaporating thin-film resistance. Our main conclusions are as follows:

1) The shape of the meniscus profile is not noticeably changed by the occurrence of evaporation.

2) The local heat flux asymptotes to a finite maximum magnitude at the tip of the meniscus cusp, the magnitude being strongly dependent on the value of the interface evaporation resistance and practically insensitive to the existence of a nonevaporating thin film at the wall.

3) The velocity at the meniscus line grows very rapidly from zero at the tip of the meniscus cusp to a maximum magnitude which, for any given $\bar{\sigma}$, is larger for smaller values of ϵ. If the interface evaporation resistance is ignored altogether ($\bar{\sigma}=2.0$), the velocity reaches physically impossible magnitudes for sufficiently small ϵ.

4) Serious errors in the value of the total meniscus Nusselt number can arise if interface evaporation resistance is ignored altogether.

References

[1] Berger, M. E. and Feldman, K. T. Jr., "Analysis of Circumferentially Grooved Heatpipe Evaporators," ASME Paper 73WA/HT-13, Winter Annual Meeting, Detroit, Mich., Nov. 1973.

[2] Schneider, G. E., Yovanovich, M. M., and Wehrle, V. A., "Thermal Analysis of Trapezoidal Grooved Heatpipe Evaporator Walls," *AIAA Progress in Astronautics and Aeronautics: Thermophysics of Spacecraft and Outer Planet Entry Probes*, edited by A. M. Smith, Vol. 56, AIAA, New York, 1977, pp. 69-83.

[3] Edwards, D. K., Balakrishnan, A., and Catton, I., "Power-Law Solutions for Evaporation From a Finned Surface," *Journal of Heat Transfer*, Vol. 96, Aug. 1974, pp. 423-425.

[4] Jakob, M., *Heat Transfer*, Vol. 1, John Wiley and Sons, New York, 1949.

[5] Sukhatme, S. P. and Rohsenow, W. M., "Heat Transfer During Film Condensation of a Liquid Metal Vapor," *Journal of Heat Transfer*, Vol. 88, Feb. 1966, pp. 19-28.

[6] Paul, B., "Compilation of Evaporation Coefficients," *ARS Journal*, Sept. 1962, pp. 1321-1328.

[7] Read, A. D. and Kitchener, J. A., "The Thickness of Wetting Films," *Wetting*, Society of Chemical Industry, S.C.I. Monograph 25, 1967.

[8] Sheludko, A., *Colloid Chemistry*, Elsevier, Amsterdam, 1966.

[9] Potash, M. Jr. and Wayner, P. C. Jr., "Evaporation from a Two-Dimensional Extended Meniscus," *International Journal of Heat and Mass Transfer*, Vol. 15, 1972, pp. 1851-1863.

[10] Sparrow, E. M. and Starr, J. B., "Heat Transfer to Laminar Flow in Tapered Passages," *Journal of Applied Mechanics*, Sept. 1965, pp. 684-689.

[11] Batchelor, G. K., *An Introduction to Fluid Dynamics*, Cambridge University Press, Cambridge, England, 1970.